Active flap control on an aeroelastic wind turbine airfoil in gust conditions using both a CFD and an engineering model

T Gillebaart [1] , L O Bernhammer[2] , A H van Zuijlen[3] and G A M van Kuik [4]

Faculty of Aerospace Engineering, Delft University of Technology, Kluyverweg 1, 2629HS Delft, The Netherlands

E-mail: t.gillebaart@tudelft.nl

Abstract. In the past year, smart rotor technology has been studied significantly as solution to the ever growing turbines. Aeroservoelastic tools are used to asses and predict the behavior of rotors using trailing edge devices like flaps. In this paper an unsteady aerodynamic model (Beddoes-Leishman type) and an CFD model (URANS) are used to analyze the aeroservoelastic response of a 2D three degree of freedom rigid body wind turbine airfoil with a deforming trailing edge flap encountering deterministic gusts. Both uncontrolled and controlled simulations are used to asses the differences between the two models for 2D aerservoelastic simulations. Results show an increase in the difference between models for the y component if the deforming trailing edge flap is used as control device. Observed flap deflections are significantly larger in the URANS model in certain cases, while the same controller is used. The pitch angle and moment shows large differences in the uncontrolled case, which become smaller, but remain significant when the controller is applied. Both models show similar reductions in vertical displacement, with a penalty of a significant increase in pitch angle deflections.

1. Introduction

Over the last years, smart rotor technology has attracted significant research interest in an effort to meet the challenges imposed by ever growing turbines. As turbines are increasing in size, traditional construction methods reach their limits and novel solutions need to be found to efficiently address the strong increase in loads and stiffness requirements modern wind turbine blades have. Several researchers have demonstrated numerically how efficiently adaptive trailing edge devices can address such load alleviation problems in the blade [1, 2] as well as in the complete turbine [3]. All of these simulations have been performed in aeroelastic software such as HAWC2 [4] and DU-SWAT [5]. Both tools use the same aerodynamic formulations, namely a blade element momentum approach combined with an implementation of the the adaptive trailing edge model that has been developed by the Danish Technical University (DTU) [6]. The basis of these models is the 2D unsteady aerodynamic model.

[1] PhD candidate, Aerodynamics
[2] PhD candidate, Wind Energy / Aerospace Structures and Computational Mechanics
[3] Assistant Professor, Aerodynamics
[4] Scientific Director DUWIND, Professor, Wind Energy

The unsteady aerodynamic model is one of the available 2D models of flapping wings. These models have a long history, dating back to the 1930s, when Theodorsen solved the flat plate problem of a wing undergoing harmonic oscillations [7]. While this model is formulated in the frequency domain, later researchers such as Leishman [8] or the French institute ONERA [9] have developed time domain models. Both of these models are valid in the linear region of the curve and aimed at airfoils without flaps. DTU has taken up the work and formulated a unsteady aerodynamic model for thin airfoils with adaptive trailing edges [10]. As this model was linear and therefore only valid in for potential flow, efforts have been made to incorporate a dynamic stall model of Beddoes-Leishman type [11]. This combined model [12, 6] has also been compared to experimental results. A series of wind tunnel tests has been performed to validate this model [1, 13]. All of these test were done in a 2 dimensional wind tunnel test set-up and a prescribed motion.

During the operation of flaps, certainly of discrete flap designs, vortices are shed from the edges. These vortices might interact with each other or the tip vortex and therefore render the assumptions underlying the blade element momentum method invalid. A way to further quantify the accuracy of engineering models is through the use of computational fluid dynamics. First efforts in using CFD for 2D controlled flap motion have been made by Heinz et al. [14]. These efforts will be followed up in this research paper by giving a thorough quantification of the aeroservoelastic response of a 3 degree of freedom structural model combined with two different aerodynamic models, namely the unsteady aerodynamic model [6] and URANS computations. As a first step, 2D simulations are used to asses the differences between the models in aeroservoelastic response to deterministic gusts. To asses this the DU91-W2-250 airfoil is used [15], where the last 10% is used as a deforming flap, which is connected to a PD controller. To limit the complexity of the controller in this research, noise, delay maximum rotational speed and maximum hinge force (known influences in the controller system) are currently not modelled. Two deterministic gust types are considered: 1-cosine and Mexican hat gust to have controlled inflow conditions, limiting the scope of this study, but ensuring interpretable results. Both uncontrolled and controlled responses are given, after which the differences between the model responses are analyzed.

2. Modeling approach of aeroservoelastic system

Two aerodynamic models are used as input to an aeroservoelastic system: 1) an unsteady aerodynamic model and 2) a high fidelity Unsteady Reynolds Averaged Navier-Stokes (URANS) model. Both models are coupled with a three degree of freedom rigid body structural model (horizontal displacement, vertical displacement and pitching) including a deformable trailing edge flap. To limit the structural response due to gusts a PD controller is used to control the flap during gusts. Both aerodynamic models, the structural model, the controller and the flow conditions are discussed in this section.

2.1. Unsteady Aerodynamic Model

The engineering model for unsteady sectional aerodynamics that can be found in HAWC2 [4] and DU-SWAT [5], has been implemented based on the description by Bergami and Gaunaa [6] and is identical to the implementation in DU-SWAT. The starting point is the steady lift curve. This curve can be obtained either experimentally or numerically. Currently, CFD model is used to generate the lift curves. This lift curve is in reality a lift surface, as not only the angle of attack (α), but also the flap deflection angle (β) is an input parameters to obtain the lift coefficient. This lift coefficient (C_l^{st}) can be separated into a linear, attached flow region over the airfoil (C_l^{att}) and a fully separated flow (C_l^{fs}) as given in Equation 1.

$$C_l^{st} = C_l^{att} f^{st} + C_l^{fs} \left(1 - f^{st}\right) \tag{1}$$

The attached lift coefficients are simply obtained by computing the lift curve slope as a function of α and β, as well as the zero lift angle of attack (α_0). The separation coefficient f^{st} is obtained by comparing the linear, attached lift coefficient C_l^{att} to the actual lift curve.

$$f^{st} = \left(2\sqrt{\frac{C_l^{st}}{C_l^{att}}}\right)^2 \tag{2}$$

This allows computing the fully separated contribution to the lift.

$$C_l^{fs} = \frac{C_l^{st} - C_l^{att} f^{st}}{1 - f^{st}} \tag{3}$$

So far, all values are steady aerodynamic solutions. To move to a dynamic domain, a quasi-steady angle of attack (α_{qs}) and a quasi-steady flap angle (β_{qs}) are obtained.

$$\alpha_{qs} = \alpha_{3/4} = \alpha_{st} - \frac{\dot{y}}{U_0} + \frac{(0.5 - \epsilon_{EA})\, b_{hc}\dot{\alpha}}{U_0} \tag{4}$$
$$\alpha_{eff} = \alpha_{qs}\Phi\left(0\right) + \sum^{N_{lag}} z_i^{\alpha}$$

$\alpha_{3/4}$ is the angle of attack at 3/4 of the chord and z is a state variable depending on the downwash time history. Φ is a lag function with experimentally obtained coefficients, ϵ_{EA} is the distance from the aerodynamic center to the elastic axis, $U_0$is the freestream velocity, y the vertical displacement and b_{hc} the half chord. For the flap deflection angle an analogue procedure is followed, which can be found in [6]. The potential lift ($C_{l,pot}$) is a sum of the circulatory and non-circulatory terms.

$$C_l^{pot} = C_l^{att}\left(\alpha_{eff}, \beta_{eff}\right) + \pi\frac{b_{hc}}{U_0}\dot{\alpha} + \frac{F_{dydx}}{\pi}\frac{b_{hc}}{U_0}\dot{\beta} \tag{5}$$

When including flow separation, the non-circulatory terms remain unchanged, while the circulatory terms get expanded by:

$$C_{l,circ}^{dyn} = C_{l,att}\left(\alpha_{eff}, \beta_{eff}\right) f^{dyn} + C_l^{fs}\left(\alpha_{eff}, \beta_{eff}\right)\left(1 - f^{dyn}\right) \tag{6}$$

To obtain the dynamic separation coefficient f^{dyn}, the both potential lift and the steady separation coefficient are passed through a first order filter. Details on this procedure can be found in [6]. The lift coefficient is the sum of the circulatory dynamic and the non-circulatory terms. The drag and moment coefficients are also based on the steady data. They are the sum of individual components that can be obtained in a straightforward manner as given [6].

$$C_d = C_d^{eff} + C_{d,ind}^{\alpha} + C_{d,ind}^{\beta} + C_{d,ind}^{f} \tag{7}$$

$$C_m = C_m^{qs} + C_m^{nc,\dot{\alpha}} + C_m^{nc,\dot{\beta}} \tag{8}$$

The flap for has been modelled with a chord length 10 percent. CFD simulations sweeping over angles of attack from -20 to 20 degrees and flap angles from -7 to 7 degrees are used to obtain the steady input data for the unsteady aerodynamic model. The same mesh, turbulence model and Reynolds numbers are used as for the unsteady CFD (URANS) model.

To include gusts in the unsteady aerodynamic model a temporal variation in the angle of attack and inflow velocity magnitude are used.

2.2. URANS model

To model the fluid around the airfoil and flap the incompressible Unsteady Reynolds Averaged Navier Stokes (URANS) equations together with the $k-\omega$ SST turbulence model are used. The equations are written in Arbitrary Lagrangian Eulerian (ALE) form and discretized using the finite volume method as implemented in OpenFOAM [16]. The equations are solved using the PISO algorithm [17], with second order spatial and temporal discretization. The URANS continuity and momentum equation in integral ALE formulation are give in Equation 9 and 10, respectively.

$$\int_{V_C(t)} (\nabla \cdot \mathbf{u})\, dV = 0 \tag{9}$$

$$\begin{aligned} \frac{\partial}{\partial t}\int_{V_C(t)} \mathbf{u} dV \;&+\; \oint_{S_C(t)} \mathbf{n}\cdot(\mathbf{u}-\mathbf{u}_m)\mathbf{u} dS \\ &-\; \int_{V_C(t)} \nabla\cdot(\nu\nabla\mathbf{u}) dV = \int_{V_C(t)} \frac{\nabla p}{\rho} dV\,. \end{aligned} \tag{10}$$

Here V_C is the control volume, S_C the surface of the control volume, $\mathbf{u}$ is the velocity vector, $\mathbf{u}_m$ the mesh velocity vector, ν the kinematic viscosity modelled by the turbulence model, p the pressure and ρ the density, which is assumed constant. The mesh velocity is determined using the Discrete Geometric Conservation Law (DGCL) and the mesh deformation. The mesh is deformed based on the motion of the structure using Radial Basis Functions (RBF) as presented in [18], resulting in a robust and efficient way of deforming the fluid mesh.

Gusts are incorporated in both the URANS model and the unsteady aerodynamic model. For the unsteady aerodynamic model gust are introduced by a change in angle of attack and velocity. For the URANS model the mesh velocity technique is used [19]. The method is based on using the mesh velocities to incorporate the gusts as shown in the Equations 11 and 12.

$$V = \mathbf{u} - \mathbf{u}_m + \mathbf{u}_g = (u - u_m + u_g)\,\mathbf{i} + (v - v_m + v_g)\,\mathbf{j} + (w - w_m + w_g)\,\mathbf{k} \tag{11}$$

$$\tilde{\mathbf{u}}_m = \tilde{u}_m\mathbf{i} + \tilde{v}_m\mathbf{j} + \tilde{w}_m\mathbf{k} = (u_m - u_g)\,\mathbf{i} + (v_m - v_g)\,\mathbf{j} + (w_m - w_g)\,\mathbf{k} \tag{12}$$

Here u, v and w are the velocity components, u_m, v_m and w_m are the geometric grid velocities caused by mesh deformations and u_g, v_g and w_g are imposed gust velocities. By modifying the grid velocities the gust velocities are incorporated in the simulation. The modified grid velocities are represented by $\tilde{u}_m$, $\tilde{v}_m$ and $\tilde{w}_m$. For global gusts, with equal velocity in whole computational domain, this is the same as moving the mesh accordingly. However, this method also gives the possibility to simulate traveling (local) gusts, which vary spatially across the domain.

2.3. Structural model

Both the URANS model and the unsteady aerodynamic model are coupled to a 3 degrees of freedom structural model without structural damping. This model is governed by the following equations:

$$m\ddot{x}_s + k_x x_s = F_x + ml\dot{\theta}_s^2 \cos(\theta_s + \theta_g) + ml\ddot{\theta}_s \sin(\theta_s + \theta_g) \tag{13}$$

$$m\ddot{y}_s + k_y y_s = F_y + ml\dot{\theta}_s^2 \sin(\theta_s + \theta_g) - ml\ddot{\theta}_s \cos(\theta_s + \theta_g) \tag{14}$$

$$\left(I_{CG} + ml^2\right)\ddot{\theta}_s + k_\theta \theta_s = F_\theta + ml\ddot{x}_s \sin(\theta_s + \theta_g) - ml\ddot{y}_s \cos(\theta_s + \theta_g) \tag{15}$$

Where, m is the mass per unit depth, k is the spring stiffness in the respective degree of freedom, F is the aerodynamic force in the respective degree of freedom, $F\theta$ is the counter clockwise positive aerodynamic moment around the rotational center, l is the distance between the centre of gravity and the rotational centre positive in the direction from leading edge to trailing edge, θ_s is pitch angle deformation, θ_g the geometric installed pitch angle and I_{CG} is the moment of inertia around the centre of gravity. The equations are solved in time by using an explicit four stage Runge-Kutta time integration. In Figure 1 an illustration is depicting the aerodynamic forces and relevant geometric variables. The model is equal to the one used in [14]. During this

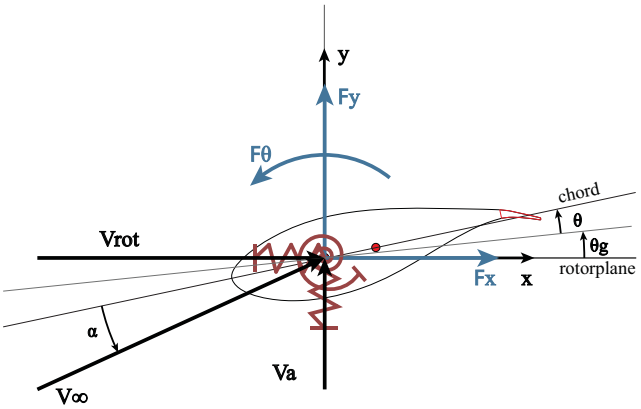

Figure 1. Illustration of structural model including a flap together with forces, inflow directions and angle definitions.

study the parameters stated in Table 1 are used in the structural model. The values stated result in a realistic 2D representation of an airfoil section in a wind turbine blade [14]. Next, the fluid and structural model need to be coupled. Coupling between the structure and aerodynamics is done in a strong way using sub iterations combined with Aitkens under relaxation [20], such that the partitioned approach has no influence on the results.

2.4. Controller and Flap

Both models use a PD controller on the body velocity to describe the rotational velocity of the flap. As input the vertical velocity and the acceleration of the body (i.e. wing) are used, with the goal of minimizing the displacement in vertical direction (y). Consequently, the rotational velocity is integrated using a second order backward differencing scheme in the URANS model and a Runge-Kutta scheme in the unsteady aerodynamics model. The controller is described by Equation 16. Noise and delay are not considered in this controller, which will be present in the actual system. However, to compare the two models these influences are considered to be less important in the current scope of the study.

Table 1. Structural properties for three degree of freedom rigid body model

c	1 m	k_x	6316 N/m
RC from LE	0.3 m	k_y	1579 N/m
CG (from LE)	0.35 m	k_θ	8290 N m/rad
m (per unit depth)	40 kg/m	θ_g	5^o
I_{CG}	2 kg m^2		

$$\frac{d\beta}{dt} = K_v \frac{dy}{dt} + K_a \frac{d^2y}{dt^2} \tag{16}$$

The gains are tuned to: $K_v = -100$ and $K_a = -20$ by hand using the unsteady aerodynamic model, which does not necessarily ensures an optimal controller.

From the integration of the rotational velocity the flap angle is obtained, which is used to deform the flap accordingly. To prevent sharp edges on the airfoil surface a smooth deformation is chosen described in Equations 17.

$$y_{flap} = y^0_{flap} - (x_{flap})^2 \beta \frac{1}{l_{flap}} \tag{17}$$

Here y_{flap} and x_{flap} are the coordinates describing the flap shape with there origin at the flap base. Additionally, y^0_{flap} is the original y position of the flap, β is the flap angle in radians, and l_{flap} is the flap length. The flap length is chosen to be 10% of the chord. No deformation in x direction is assumed, which is valid for small angles. The maximum allowed angle in the controller is 7 degrees (0.12 rad), which makes this assumption reasonable for the intended purpose. In Figure 2 the flap deformation is shown.

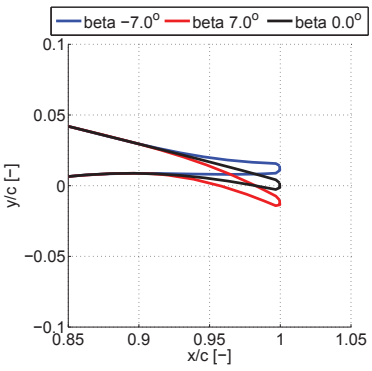

Figure 2. Flap deformation

2.5. Flow conditions and gusts

Typical flow conditions for a wing turbine section close to the tip are taken from [14]. A rotational velocity of 60 m/s is chosen, while as unperturbed axial velocity a speed of 10 m/s is used. With a chord length of 1 m and the dynamic viscosity equal to $1.4531 \cdot 10^{-5}$ m^2/s a

Reynolds number of 4.19 million is obtained. For the turbulence model a turbulence intensity of 0.01% is used. The DU91-W2-250 airfoil is used as typical wind turbine airfoil [15], where the last 10% of the wing are used as flap.

To trigger a clear well defined response prescribed gusts are used. Two types of gusts are considered: a 1-cos gust and a Mexican hat gust. Equations 18 and 19 describe the 1-cos and Mexican hat gusts, respectively.

$$V^g_{cos}(t) = \frac{A_g}{2}\left(1 - \cos\left(2\pi f_g \xi\right)\right) \text{ if } 0 < \xi < 1/f_g \tag{18}$$

$$V^g_{mex}(t) = \frac{A_g}{2}\left(1 - \cos\left(2\pi f_g \xi\right)\right)\sin\left(3\pi f_g \xi\right) \text{ if } 0 < \xi < 1/f_g \tag{19}$$

Here V_g is the gust velocity in time and space, A_g the gust amplitude, f_g the gust frequency and $\xi = t - t^g_0$, where t^g_0 is the starting time of the gust. During this study only gusts in axial direction are considered.

3. Results

With the two models discussed in previous sections the airfoil response to two gusts are simulated and the results are compared. The computational times (CPU time) for one of these simulations are $O(10)$ seconds and $O(50)$ hours for the unsteady aerodynamic model and URANS model, respectively. Results are shown with respect to their steady state values, which are stated in Table 2. Here Cms_θ is the moment coefficient around the rotational center, counterclockwise positive. A cosine and Mexican hat gust with a frequency of 1.2 Hz and an amplitude of 1 m/s

Table 2. Steady state forces and deflections for both the URANS and UA model.

	URANS	UA
x [m]	-0.036	-0.039
C_x	-0.101	0.107
y [m]	0.992	1.026
C_y	0.691	0.715
θ [deg]	1.124	1.191
Cms_θ	0.072	0.076

are chosen. In addition to the airfoil with controller also the uncontrolled cases are simulated to determine the decrease in vertical displacement. In Figure 3 and 4 the dynamic response of the airfoil to a cosine gust and Mexican hat gust is shown for both models with and without controller. On a global level both models perform similar: they reduce the maximum deflection of the airfoil significantly. However, important differences can be found in both the level of reduction, flap deflection and the consequences of this deflection, on which the next sections elaborate.

3.1. Uncontrolled response

First the response without controller is compared for both models. Significant differences can be found in all displacement and force variables. The focus will be on the force and displacement in y and the pitching moment and angle, since these are the most critical values when looking at the controlled case. Differences are the (absolute) maximum amplitude differences of the response normalized by the band of the URANS response, stated in percentage. In Table 3

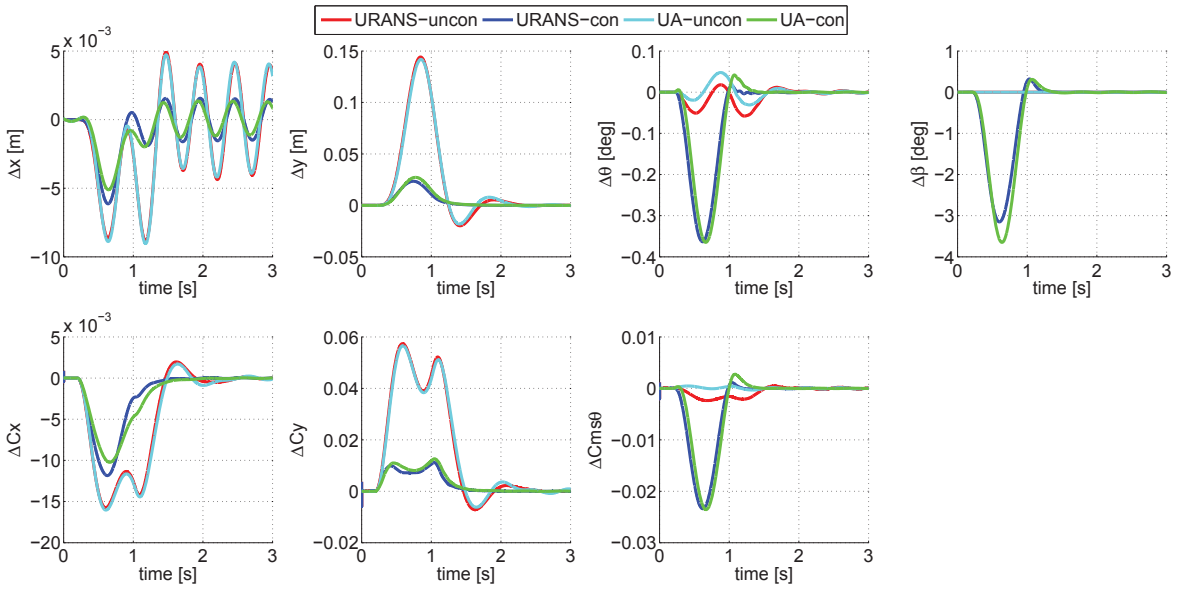

Figure 3. Response in time to a 1-cos gust with amplitude 1 m/s and frequency of 1.2 Hz for the unsteady aerodynamic (*UA*) model and the URANS model (*URANS*) for both the uncontrolled (*uncon*) and controlled case (*con*)

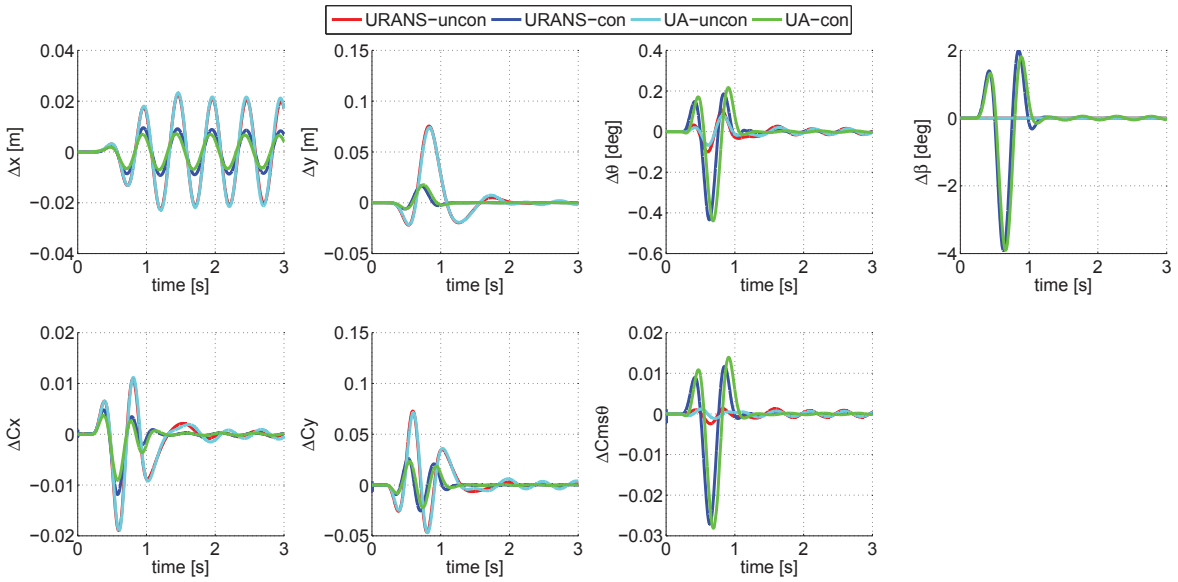

Figure 4. Response in time to a Mexican hat gust with amplitude 1 m/s and frequency of 1.2 Hz for the unsteady aerodynamic (*UA*) model and the URANS model (*URANS*) for both the uncontrolled (*uncon*) and controlled case (*con*)

the differences are given for both the gusts in controlled and uncontrolled conditions. As seen in Table 3 both the vertical force and displacement are close to each other with differences between 1.4% to 1.7%. Similar behavior is found in the horizontal component of the force and displacement, with differences between 1.2% and 1.4%. Although the difference in the vertical and horizontal paramaters are small, the difference in moment and pitch angle are relatively big.

Both the moment and the pitching angle have differences up to -57.7%. Even though this is a large relative difference, in absolute terms its rather minor (e.g. 0.03^o in pitch angle). Besides the large (relative) differences in the pitch angle and moment both models behave very similar in amplitude response.

Table 3. Differences between the unsteady aerodynamic model and URANS model in the gust responses of a smart airfoil. Difference are given in normalized maximum amplitude differences relative to the URANS results. Normalization is done by the band of the URANS response of the respective variable.

	Cosine		Mexican hat	
variable	**uncontrolled**	**controlled**	**uncontrolled**	**controlled**
x	1.2%	-12.7%	1.3%	10.7%
C_x	1.4%	-12.5%	0.0%	-14.4%
y	1.6%	-16.5%	1.7%	-6.6%
C_y	1.4%	-8.9%	1.4%	3.8%
θ	-35.9%	0.9%	-15.8%	3.3%
Cms_θ	-57.7%	1.1%	-34.7%	5.3%
β	-	-14.8%	-	2.1%

3.2. Controlled response

Adding a controller, and thus a moving trailing edge flap, increases complexity, which both models handle differently. First, it is clear from both models that a significant reduction in vertical displacement can be achieved: 83% for the URANS model and 81% for the unsteady aerodynamic model in case of the cosine gust. Considering the Mexican hat gust a reductions of 78% and 75% are found, respectively. The consequence of the flap actuation is an increase in both the moment and the related pitch angle. A deflection of the flap causes an additional force far away from the rotational centre, causing an steep increase in the moment. However, the unsteady aerodynamic model predicts a larger change in pitch moment and angle when compared to the URANS model, while a smaller maximum flap angle is used.

As for the uncontrolled response, the responses of the two models are compared to asses the magnitude of the differences. For y the difference increased up to -16.5% for the Mexican hat gust, while differences in C_y are up to -8.9%. These relative differences are significantly larger than the ones in the uncontrolled case. However, the difference for the pitch angle and moment (θ and Cms_θ) decreased compared to the uncontrolled case, to values up to 5.3%. Even though the amplitude differences decreased, phase differences can be observed in both the uncontrolled and controlled cases. Additionally, when studying the URANS results higher frequency vibrations can be found in θ for the cosine gust. Finally the flap angle shows a significant difference for the cosine gust: -14.8%. Surprisingly, there is no significant difference in maximum flap angle for the Mexican hat gust.

4. Conclusion

In this study two aerodynamic models are used to simulate the aeroservoelastic response of a smart wind turbine airfoil: the unsteady aerodynamic model and the URANS model. The goal of this study is to give a thorough quantification of the aeroservoelastic response of a 3 degree of freedom structural model, while comparing the two different aerodynamic models. This is done by assessing the controlled and uncontrolled response to typical gusts.

Comparing the structural and aerodynamic response for the uncontrolled case indicates that the relative difference are small for the vertical components (1.4 to 1.7%), while for the pitching

angle and moment the relative difference are significantly larger (up to -57.7%). However, it must be noted that the absolute differences in the dynamic response for these parameters are small. For the controlled case an increase in difference compared to the uncontrolled cases is found in the vertical displacement and force: 3.8% to -16.5%. Also the flap angle shows similar differences: -14.8%. The pitching angle and moment do have a significant smaller relative difference (up to 5.3%). It can be concluded that for the investigated cases the differences increase for the controlled direction (y) when a flap and controller are added. However, pitch response is very similar in amplitude in the controlled cases. In phase and in post gust response differences can still be found.

Finally, both models do predict a similar reduction in vertical displacement: 83 and 81% for the cosine gust and 78 and 75% for the Mexican hat gust. However, due to the flap deflection a significant increase in pitching moment and angle is observed. This has also been observed in other studies.

Two gusts are considered in this study, which already show a wide range of differences. From these inflow conditions it can be seen that in uncontrolled cases the observed behavior in amplitude is similar for both models. Differences in pitch and moment response are significantly different. Also depending on the type of gusts considered, the differences between models do vary. Therefore a more detailed comparison will be done, using a wider range of gusts and other inflow conditions, such as a turbulent inflow. Additionally, more attention must be given to the flap and its controller by including maximum rotational speed, delays, signal noise and maximum allowed (achievable) forces in the system.

References

[1] Baek P 2011 *Unsteady Flow Modeling and Experimental Verification of Active Flow Control Concepts for Wind Turbine Blades* (DTU RISO) phD Thesis
[2] Andersen P 2010 *Advanced Load Alleviation for Wind Turbines Using Adaptive Trailing Edge Flaps: Sensoring and Control* (DTU RISO) phD Thesis
[3] Bernhammer L, Breuker R D and van Kuik G 2013 Assessment of fatigue and extreme load reduction of hawt using smart rotors *Proceedings of the 9th PhD Seminar on Wind Energy in Europe* (Visby, Sweden: EAWE)
[4] Larsen T and Hansen A 2012 How 2 hawc2, the user's manual Risø-r-1597(ver. 4.3)(en)
[5] Bernhammer L, Breuker R D and van Kuik G 2012 Du-swat: A new aeroelastic horizontal axis wind turbine analysis tool *Proceedings of the 8th PhD Seminar on Wind Energy in Europe* (Zurich, Switzerland: EAWE)
[6] Bergami L and Gaunaa M 2012 Ateflap aerodynamic model, a dynamic stall model including the effects of trailing edge flap deflection Risø-r-1792(en)
[7] Theodorsen T 1934 General theory of aerodynamic instability and the mechanism of flutter Naca report 496
[8] Leishman J 1994 *Journal of Aircraft* **31** 288–297
[9] McAlister K, Lambert O and Petot D 1984 Application of the onera model of dynamic stall 2399 NASA Technical Paper
[10] Gaunaa M 2007 *Wind Energy* **13** 167–192
[11] Leishman J and Beddoes T 1986 A generalized model for airfoil unsteady aerodynamic behaviour and dynamic stall using indicial method *Proceedings of the 42nd Annual Forum of the American Helicopter Society* (Washington D.C., USA)
[12] Andersen P, Gaunaa M, Bak C and Hansen M 2009 *Wind Energy* **12** 734–751
[13] Bak C, Gaunaa M, Andersen P, Buhl T, Hansen P and Clemmensen K 2010 *Wind Energy* **13** 207–219
[14] Heinz J, Sørensen N and Zahle F 2011 *Wind Energy* **14** 449–462
[15] Timmer W A and van Rooij R P J O M 2003 *Journal of Solar Energy Engineering* **125** 488–496
[16] Jasak H 1996 *Error Analysis and Estimation for the Finite Volume Method with Applications to Fluid Flows* (Imperial College of Science, Technology and Medicine) phD Thesis
[17] Issa R 1985 *Journal of Computational Physics* **62** 40–65
[18] de Boer A, van der Schoot M and Bijl H 2007 *Computer & Structures* **85** 784–795
[19] Singh R and Baeder J D 1997 *Journal of Aircraft* **34** 465–471
[20] Mol D P and Wall W A 2001 Partitioned analysis schemes for the transient interaction of incompressible flows and nonlinear flexible structures *Trends in Computational Structural Mechanics* (Schloss Hofen, Austria: International Center Numerical Methods Engineering)